Annealing Effects on Defect Levels of CdTe:Cl Materials and the Uniformity of the Electrical Properties

M. Ayoub, M. Hage-Ali, J. M. Koebel, A. Zumbiehl, F. Klotz, C. Rit, R. Regal, P. Fougères, and P. Siffert

***Abstract*—CdTe crystals grown by the traveling heater method (THM) often show a pronounced nonuniformity along the ingots due to the thermal irregularities, the Te-excess growth conditions resulting from the retrograde slope of the solidus line of the phase diagram, and from the introduced impurities. In addition, structural defects can be present that influence the electrical and optical properties.**

The aim of this work is to study the annealing effects of Cl-doped CdTe on the uniformity of the material, the defects, the resistivity, the $\mu\tau$ product, and on the detection properties.

Samples have been annealed under various pressures (vacuum, argon, $CdCl_2$) and include different temperature stages between 250 °C and 850 °C. An increase of the resistivity was observed after a thermal treatment of these samples under argon pressure. In this case, the highest resistivity was obtained by annealing samples at 460 °C. The presence of $CdCl_2$ during the annealing leads to a better uniformity of the materials.

The defects present in the materials have been investigated by photo-induced transient current spectroscopy (PICTS), thermo-electric emission spectroscopy (TEES), and thermally stimulated current (TSC) methods, which allow the calculation of their activation energy, their cross section, and their concentration. A strong correlation between the 0.6 and 0.76 eV levels and the measured resistivity has been observed. The effects of the other levels on the electrical properties is described. A discussion about the origin of these defects and a comparison with obtained results by the above methods is then given.

***Index Terms*—Annealing, CdTe, defects, homogeneity, performance detection, photo-induced transient current spectroscopy (PICTS), resistivity, thermally stimulated current (TSC), thermo-electric emission spectroscopy (TEES), $\mu\tau$ product.**

I. Introduction

CdTe:Cl is well known as a semiconductor material used in γ and X-ray detection and other kinds of applications. But it suffers from the nonhomogeneity of the material due on the one hand to the thermal traveling heater method (THM) growth conditions, which induces the formation of Te precipitates owing to the retrograde CdTe phase diagram [1] and, on the other hand, to the impurities introduced during the growth. To understand the effects of the thermal treatment on the materials and, thus, on its homogeneity, several annealing cycles were carried out under different pressures. In this work, we are interested in the effects of the annealing on the material uniformity, the resistivity, the $\mu\tau$ product and on the radioactive detection characteristics. We therefore seek a possible correlation with the defects present in the samples that are identified by photo-induced transient current spectroscopy (PICTS), thermally stimulated current (TSC), and thermo-electric emission spectroscopy (TEES) methods.

Manuscript received November 20, 2001; revised February 27, 2002. The work of one of the authors, M. Ayoub, was supported by a Grant from the CNRS-L (National Scientific Research Center-Lebanon).

M. Ayoub is with the PHASE Laboratory, F67037 Strasbourg Cedex 2, France, and also with Louis Pasteur University, F67000 Strasbourg, France (e-mail: ayoub@phase.c-strasbourg.fr).

M. Hage-Ali, J. M. Koebel, A. Zumbiehl, F. Klotz, C. Rit, R. Regal, and P. Siffert are with the PHASE Laboratory, F67037 Strasbourg Cedex 2, France.

P. Fougères is with EURORAD II-VI, F67037, Strasbourg Cedex 2, France (e-mail: fougeres@phase.c-strasbourg.fr).

Digital Object Identifier 10.1109/TNS.2003.809981

II. Experimental Procedure

Several Cl doped CdTe samples with a size of $10\times10\times2$ mm^3 were used in order to undergo different kinds of thermal treatment. The samples were first etched with a Br-methanol solution and then placed in evacuated quartz ampoules. The thermal treatment cycles were carried out in the furnace tube. Many stages of annealing temperatures were used ranging between 250 °C and 850 °C. The annealing was carried out under different pressures (vacuum, argon, and $CdCl_2$).

All the electrical properties were systematically measured before and after the sample annealing. The $\mu\tau$ product of the electrons and the holes were calculated by the improved Hecht relation [2], the detection performance by using ^{57}Co source, the energy and the cross section of the defects were measured by PICTS (the excitation wavelength used was ($\lambda = 820$ nm)). The trap concentrations were calculated by PICTS and then corrected by the combination of the PICTS and SCLC methods [3]. The results were compared to those of TSC and TEES methods by illuminating the samples with He–Ne laser light at a wavelength of 0.63 μm.

III. Results and Discussion

The electrical characterization of the deep levels in the CdTe:Cl samples investigated before and after annealing, revealed the existence of nine different traps labeled P1, P2, P3, P4, P5, P6, P7, $P9_0$, $P9_1$. Their activation energy and their apparent capture cross sections are reported in Table I.

A. Annealing Under Vacuum

The CdTe:Cl samples were annealed at various temperature stages varying between 250 °C and 850 °C in order, on the one hand, to study the annealing effects on the evolution of the defect levels and the uniformity of the electrical properties and,

TABLE I
ENERGY AND CAPTURE CROSS SECTIONS OF THE DEEP LEVELS FOUND IN THE INVESTIGATED SAMPLES

Defects	P1	P2	P3	P4	P5	P6	P7	$P9_0$	$P9_1$
E (eV)	0.14	0.21	0.32	0.4	0.52	0.6	0.76	0.86	0.9
σ (cm^2)	$1.2x10^{-16}$	$2.3x10^{-16}$	$3.5x10^{-16}$	$1.6x10^{-14}$	$7x10^{-14}$	$8x10^{-14}$	$5x10^{-13}$	$2x10^{-12}$	$8.8x10^{-11}$

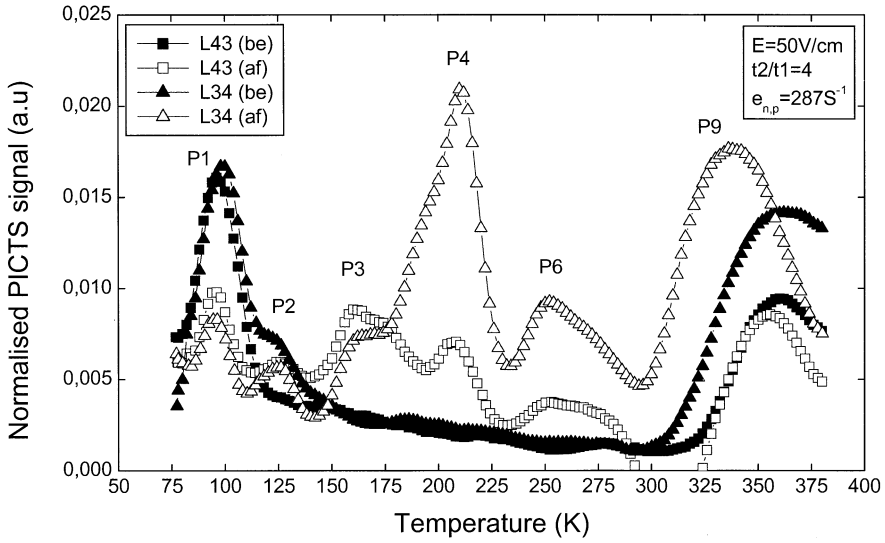

Fig. 1. PICTS defect spectra: L43(be) and L34(be) samples before annealing, L43(af) and L34(af) samples after annealing at $\mathrm{T} = 460$ °C and under vacuum.

TABLE II
DEFECT CONCENTRATIONS BEFORE AND AFTER ANNEALING SAMPLES (UNDER VACUUM)

Levels	L43		L34	
	Level concentrations (cm^{-3})			
	Before annealing	After annealing	Before annealing	After annealing
P1	$1.2x10^{13}$	$1.08x10^{13}$	$1.2x10^{13}$	$9.9x10^{12}$
P2	-	$5.74x10^{12}$	$2.6\ 10^{12}$	$5.1x10^{12}$
P3	-	$6.8x10^{12}$	-	$6.38x10^{12}$
P4	-	$7.87x10^{12}$	-	$1.89x10^{13}$
P6	-	$4.04x10^{12}$	-	$7.65x10^{12}$
P9	$1.29\ 10^{14}$	$3.6x10^{13}$	$3.35x10^{13}$	$6.38\ 10^{13}$

on the other hand, to optimize a thermal treatment for our CdTe materials.

Six deep defects were identified after annealing the samples at $\mathrm{T} = 460$ °C (Fig. 1). The levels P1 and P9 are detected before and after the annealed samples. But, the P2 level is only present in sample L34 both before and after the sample annealing. The P1 concentration decreases after the annealing while the P9 rises slightly in L34 and decreases in sample L34 (Table II).

Some new defects appear and are identified clearly after the annealing such as P3, P4, and P6. In fact, the dissociation of the P1 complex level $(\mathrm{V_{Cd}} - \mathrm{C_{Te}} - \mathrm{M})$ [4] and then the dissociated impurities during the thermal treatment induce the apparition of the defect band (0.3–0.6 eV). This band has different level concentrations between the two annealed samples, which induces the difference in the electrical properties on the two latter samples (Table III). We note that the P4 and P6 level concentrations are lower in sample L43 than L34, in which the resistivity is lower in this sample than L43. The $\mu_{\mathrm{n}}\tau_{\mathrm{n}}$ product decreases after the annealing for the two samples while the $\mu_{\mathrm{p}}\tau_{\mathrm{p}}$ product is unchanged for sample L43 and decreases slightly in sample L34.

Fig. 2 shows the detection spectra before and after annealing. The counting rates for identical conditions decreases and the detector performance degrades and polarizes after 1–5 min with an applied voltage.

However, all the annealing carried out under vacuum with various temperatures (T) lead to a deterioration of the detector as well as that of the electrical properties. In fact, this type of annealing therefore induces the formation of the vacancy defects

TABLE III
RESISTIVITY AND $\mu\tau$ PRODUCTS BEFORE AND AFTER ANNEALING SAMPLES (UNDER VACUUM)

	Resistivity (Ω.cm)		μτ (cm²/V)	
Samples	Before annealing	After annealing	Before annealing $\mu_n\tau_n$; $\mu_p\tau_p$	After annealing $\mu_n\tau_n$; $\mu_p\tau_p$
L43	$2.8\times10^{+9}$	$2\times10^{+9}$	1.5×10^{-3} ; 4×10^{-5}	7×10^{-4} ; 4×10^{-5}
L34	$3.01\times10^{+9}$	$3.3\times10^{+8}$	1.8×10^{-3} ; 3×10^{-5}	5×10^{-4} ; 4×10^{-5}

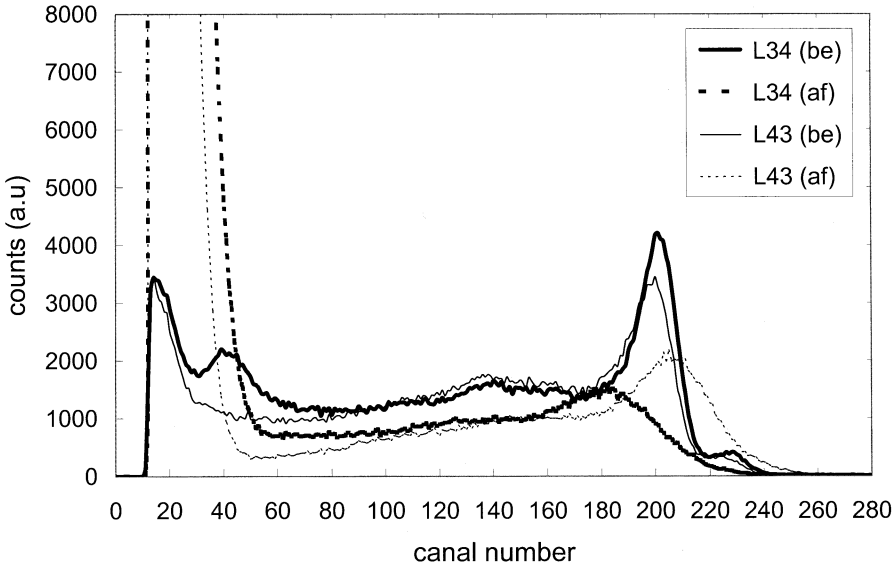

Fig. 2. ^{57}Co spectra with different detectors: L34(be) and L43(be) samples before annealing, L34(af) and L43(af) samples after annealing at $T = 460$ °C and under vacuum.

such as V_{Cd}, V_{Te} due to the difference of the partial pressure between the Cd and the Te and the presence of others kinds of defects such as the impurities (Au, In, Ag...). To avoid or minimize the formation of vacancy defects, annealing was then carried out under Argon pressure.

B. Annealing Under Argon Pressure

The same temperature stages under vacuum pressure were used varying between 250 °C and 850 °C. The samples were annealed under argon pressure. This type of annealing results in an apparition of some new defects P3, P4, P6, and P7 in addition to the variation of the following levels: P1, P2, and P9. Fig. 3 illustrates well an example of the defects found in the same samples before and after annealing at temperature stage T:700 °C, and were identified by PICTS, TSC, and TEES methods. Four levels: P1, P2, P3, and P4 are confirmed by these two latter methods. The TEES spectra show that this defect band is a hole trap. We note that some defects appear in the PICTS method and not in the TSC and the TEES methods and that the deep levels have energy that is higher than 0.6 eV. This limits the performance to identify the deep levels. The defect variation instead of the different temperatures is shown in Fig. 4, where the P6 and P7 levels appear in the ranges: 350 °C to 420 °C and 500 °C to 850 °C. The variation of these defect concentrations influences the material resistivity (Fig. 5). However, a high resistivity value was obtained at T:460 °C ($\rho = 8\times10^9$ Ω.cm, while the mean resistivity before the annealing was $1-2\times10^9$ Ω.cm). In this case, the level P6 and P7 are not present. Out of this temperature stage the resistivity decreases.

Fig. 5 shows then that the concentration of both P1 and P9 level band increases after annealing. In fact, the annealing where $T > 500$ °C or $T < 420$ °C cause a decrease in resistivity, which mean a loss of the compensator (Cl). We could then assume that there is an out diffusion of this chlorine from the Te sites. However, this hypothesis is less plausible, in favor of cadmium vacancy and metal diffusion, especially at high temperature, in the form of $CdCl_2$ that induces the formation of V_{Cd} and V_{Te} and thus the decrease in resistivity. The presence of these defects plays an important role in the compensation process (see the section on defects). On the other hand, the $\mu\tau$ product of electrons and holes are, therefore, like the resistivity, affected by the thermal treatment (Fig. 6). The high $\mu\tau$ product of electrons and holes were obtained at T:480 °C and out of this temperature stage the $\mu\tau$ product decreases. Therefore, we see clearly in the same figure that the $\mu\tau$ product decreases strongly when (T) rises.

The same phenomena appears by measuring the pulse height of the 122 KeV γ-ray with a ^{57}Co source instead of the temperature (T). In the T:460–480 °C range, the pulse height of the 122 KeV γ-ray is the better one, out this range this pulse decreasing (Fig. 7). This behavior can be explained by the appearance of new defects outside of this range with a high concentration and a high trapping time of the carriers. This leads to a degradation in the electrical properties of the materials.

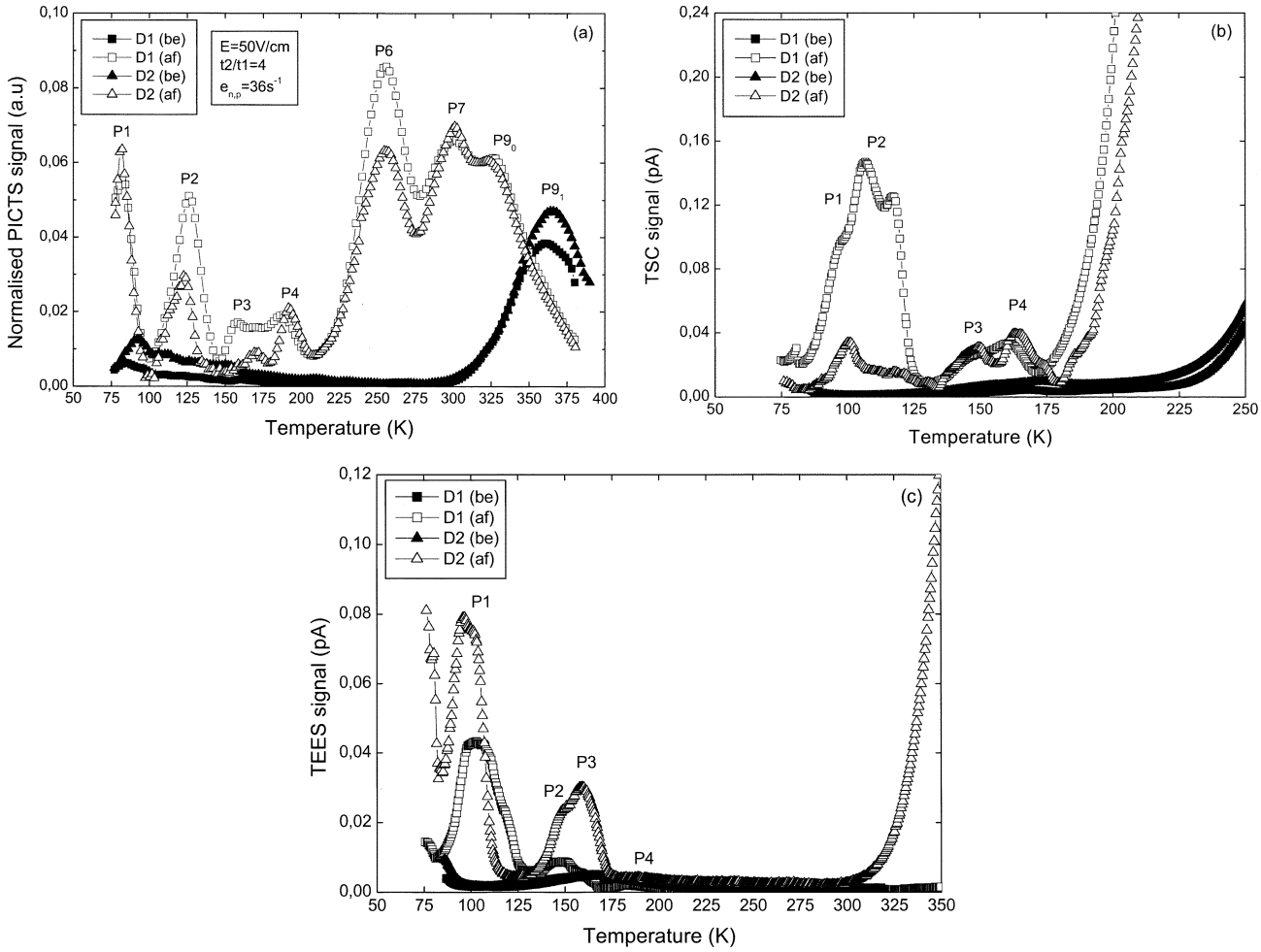

Fig. 3. PICTS, TSC, and TEES defect variations. (a) D1(be) and D2(be) samples before annealing. (b) D1(af) and (c) D2(af) samples after annealing at $T = 700\ ^{\circ}C$ and under argon pressure.

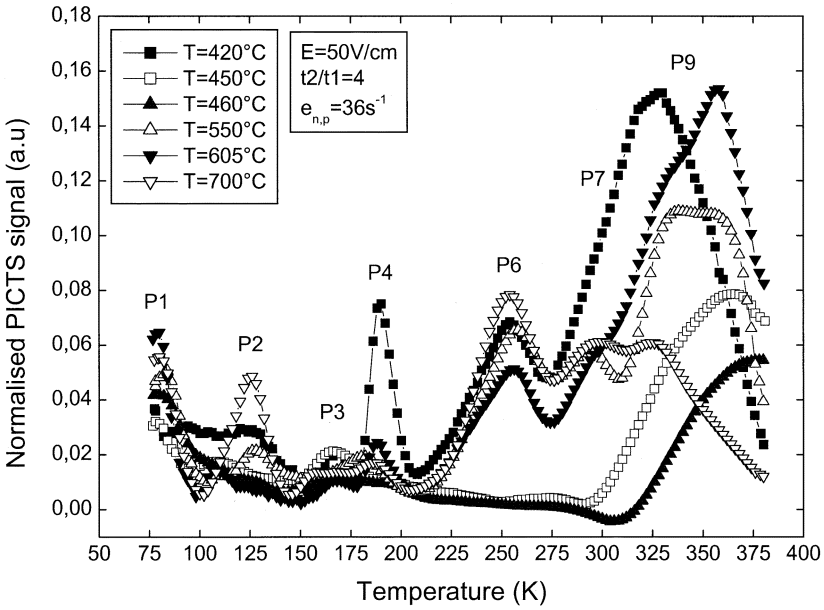

Fig. 4. PICTS defect spectra versus different annealing temperature (T).

Fig. 8 shows the detection spectra variation for different samples after annealing at the optimal temperature range. We see that after annealing some samples improve in their γ-ray performance as well as in the resistivity. The difference in the de-

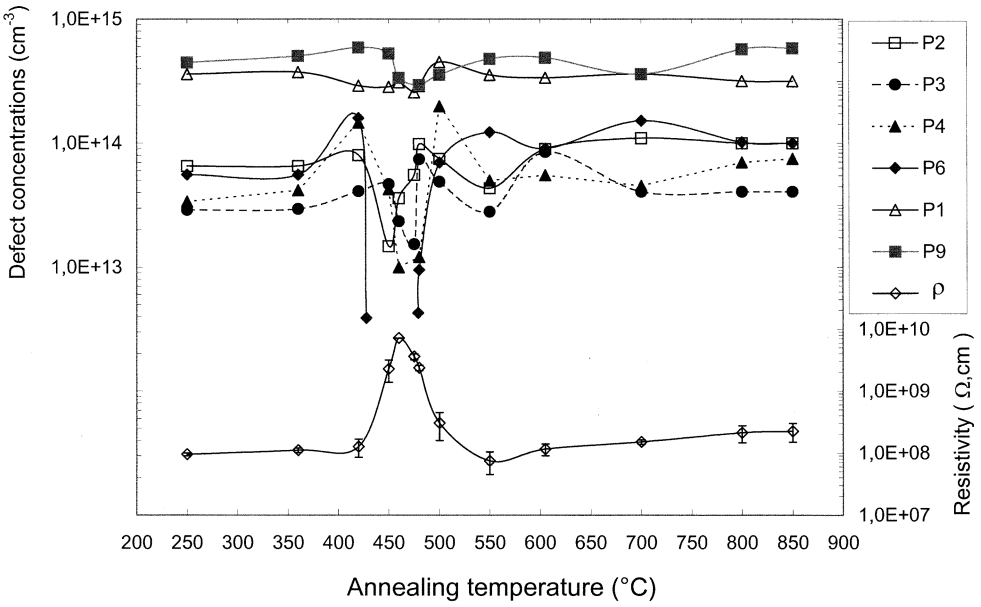

Fig. 5. Defect concentrations and resistivity variations versus annealing temperature (T).

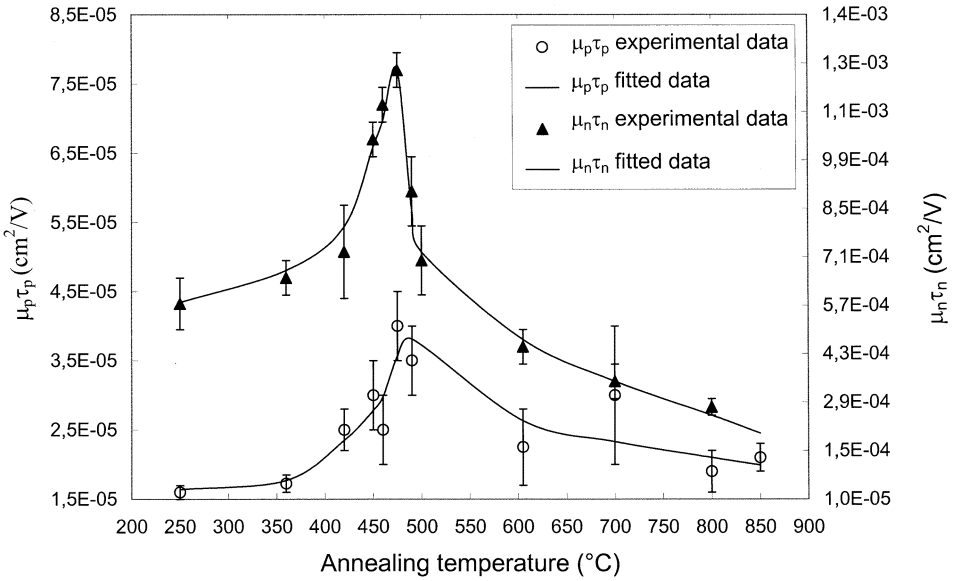

Fig. 6. Variation of $\mu\tau$ product of electrons and holes at different annealing temperatures (T).

tection spectra shows that even if we have some homogeneity, the materials are still not sufficiently uniform after these thermal treatment conditions.

C. Annealing Under $CdCl_2$

The temperature stages used annealing under $CdCl_2$ pressure are the same ones used as with annealing under argon pressure in which the resistivity obtained was the highest $(T = 460\,^{\circ}C)$. The duration of the thermal treatment is between 15 and 20 h. Several samples are annealed with different $CdCl_2$ concentrations (0.02 ppm–10 000 ppm in weight of the CdTe wafer).

Fig. 9 shows the defects detected before and after annealing with different $CdCl_2$ concentrations (10 000, 80, and 4.4 ppm) by using the PICTS and TEES methods. The P9 and P2_P3 band levels increase, and P6 disappears after annealing with 4.4 ppm of $CdCl_2$ concentration [Fig. (9a) and (b)]. Under a high $CdCl_2$ concentration ($>$80 ppm) the detectors are deteriorated and then the resistivity decreases (10^3 to 10^5 Ω.cm) (Fig. 10), in this case, PICTS and TSC spectra measurement is not possible but TEES spectra show an donor level at an energy of 0.52 eV and a weak P2_P3 acceptor level band intensity. This can be explained as chlorine doping [Fig. (9c)], especially since the conductivity of the material changes and becomes n-type. If the $CdCl_2$ continues to rise ($>$1000 ppm) the P5 level disappears but the P3 and P4 level intensities increase strongly. In this case, the metallic impurities contained in the low purity $CdCl_2$ that was used can operate and create these types of defects [Fig. (9d)]. For low $CdCl_2$ concentrations varying between 0.02–20 ppm, the resistivity is very high $(1{-}2{\times}10^9\,\Omega.\mathrm{cm})$. This

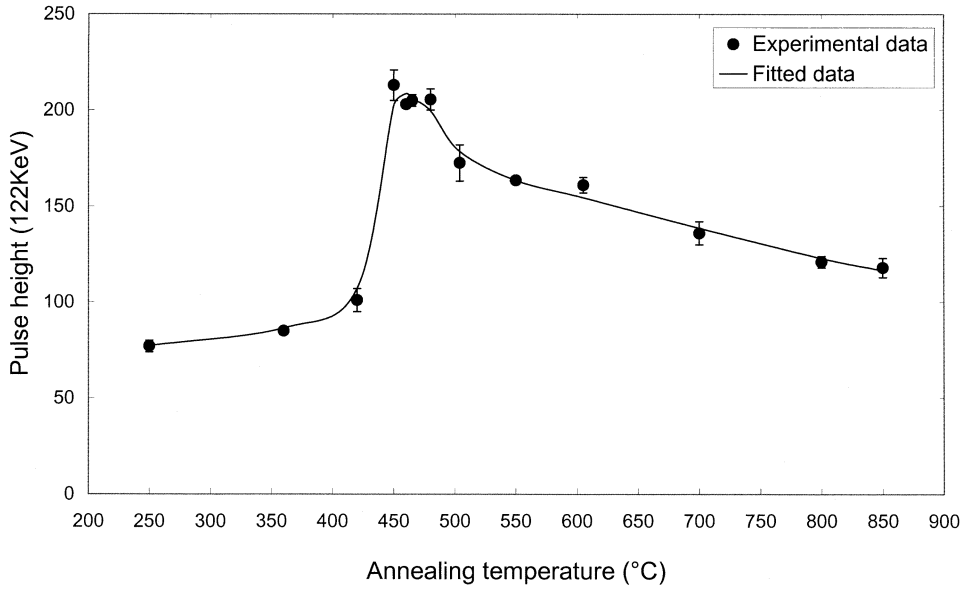

Fig. 7. Variation of the pulse height of 122 KeV γ-ray versus annealing temperature (T).

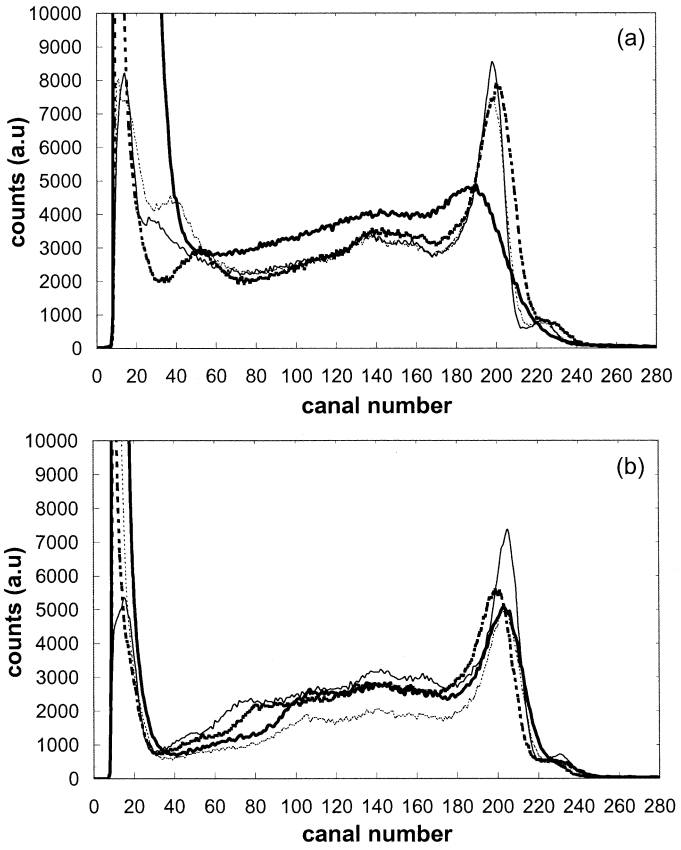

Fig. 8. $^{57}\mathrm{Co}$ spectra in different detectors (a) before annealing and (b) after annealing at T:460 °C and under Argon pressure.

fact indicates that compensation is very much involved. Outside of this concentration range the resistivity decreases (Fig. 10).

The $\mu_{\mathrm{p}}\tau_{\mathrm{p}}$ and $\mu_{\mathrm{n}}\tau_{\mathrm{n}}$ products present a clear variation with the $\mathrm{CdCl_2}$ concentration but decreases when the $\mathrm{CdCl_2}$ concentration rises above few ppm (Fig. 11). At 2.2 ppm of $\mathrm{CdCl_2}$ concentration the detection performance of the detectors investigated are similar (Fig. 12) as well as that of the resistivity $(1.5 - 2 \times 10^9\ \Omega.\mathrm{cm})$.

D. Defects in CdTe

The results obtained before and after annealing and under different pressures can help in the identification of some defects, which vary with the type of the thermal treatment. The energy and the concentration defects were calculated by PICTS and some were confirmed by TSC. By using the TEES method, it was possible to determine if the level was a hole or an electron trap. Here, we attempt to make a comparison of the detected deep traps and their possible assignation with those found in the literature, which is reported as the following.

Level P1: This level is located at $\mathrm{E_v} + 0.14$ eV and is always present in CdTe:Cl both before and after annealing. It is attributed to a complex such as $(\mathrm{In_{Cd}} - \mathrm{V_{Cd}})$ or $\mathrm{Te_i}$ [5]–[7]. Meyer *et al.* [8] have identified the $\mathrm{V_{cd}} - \mathrm{Cl_{Te}}$ acceptor complex at 0.12 eV using photoluminescence and optically detected magnetic resonance (ODMR) techniques, as well as Suzuki *et al.* [9] at 0.14 eV. Fiederle *et al.* [10] found the same complex in the 0.14–0.17 eV band. In fact, this defect level, usually called the A center, plays a significant role in the compensation process of CdTe:Cl as it seems to be the shadow of a deep donor level, which neutralizes the $\mathrm{V_{Cd}}$ native acceptor.

Level P2: This is identified at $\mathrm{E_v} + 0.2$ eV and is sometimes present in higher concentration for annealed samples. It is attributed to be $\mathrm{V_{Te}}$ [11], [12]. The same authors attributed this level later to the $\mathrm{Te_{Cd}}$ anti-site, while Zaychoskii *et al.* [13] have attributed it to Fe. The two latter explanations seem the more plausible in our case.

Level P3: This is found at $\mathrm{E_v} + 0.32$ eV and has been identified in the annealed samples. It is a candidat to the $\mathrm{Te_{Cd}}$ anti-site level possibly introduced during the growth process [4]. Other authors attribute the defect band with an activation energy varying between (0.27–0.35 eV) to metal impurities such as (Cu, Ag, Au, Pb...) [5], [7]. Hage Ali *et al.* [14] have attributed this energy band to Cu contamination by comparing the electrical behavior with the Cu and the 0.33-eV level concentrations. This hypothesis could be supported by our findings such as level P3. The dissociation of complex levels or

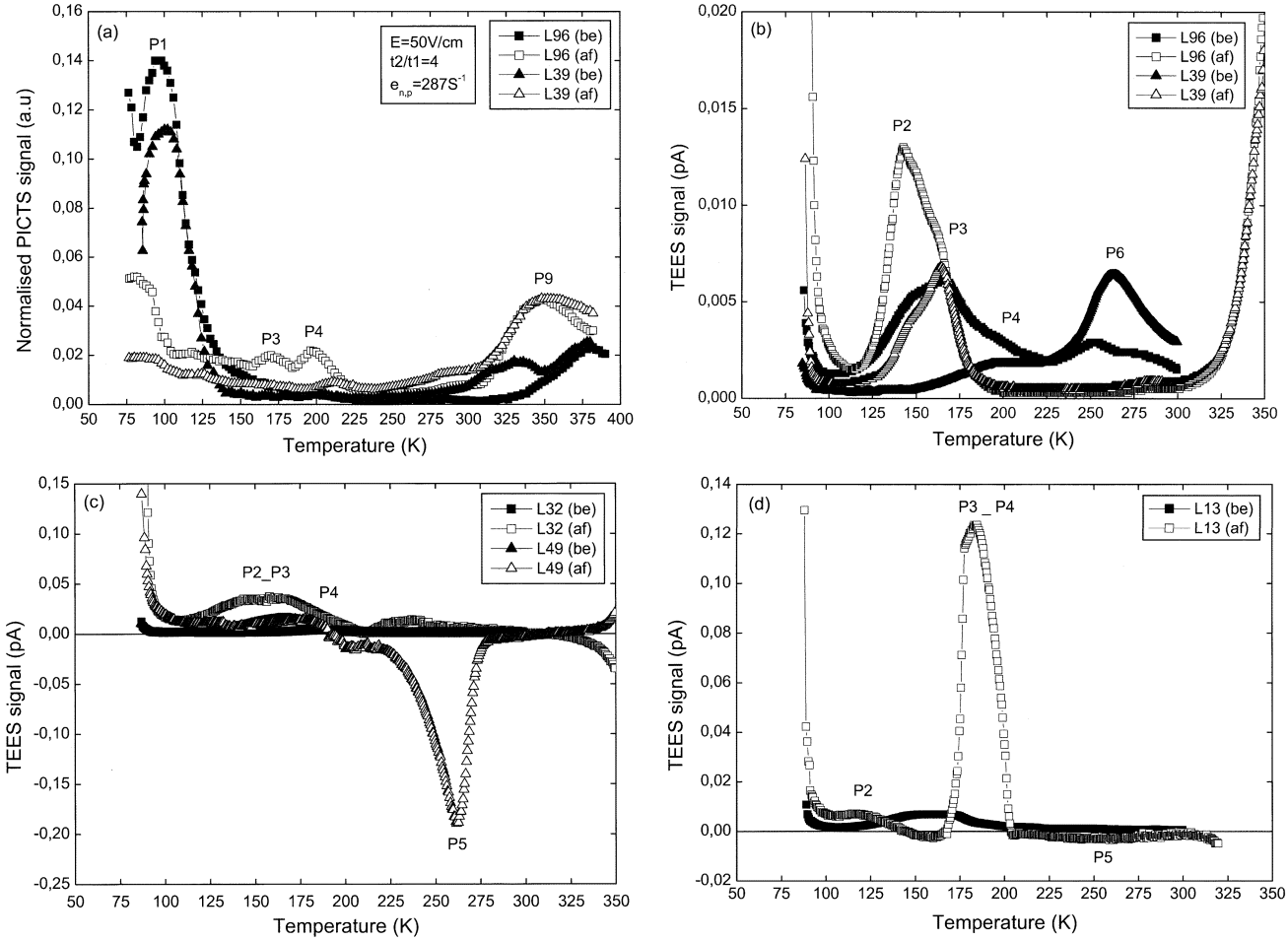

Fig. 9. Defect spectra before (be) and after (af) annealing samples (under $CdCl_2$ pressure). PICTS and TEES spectra of L96 and L39 samples (a) before and (b) after annealing with $CdCl_2$ concentration of 4.4 ppm. TEES spectra of different samples before and after annealing with $CdCl_2$ concentration of (c) 80 ppm and (d) 10 000 ppm.

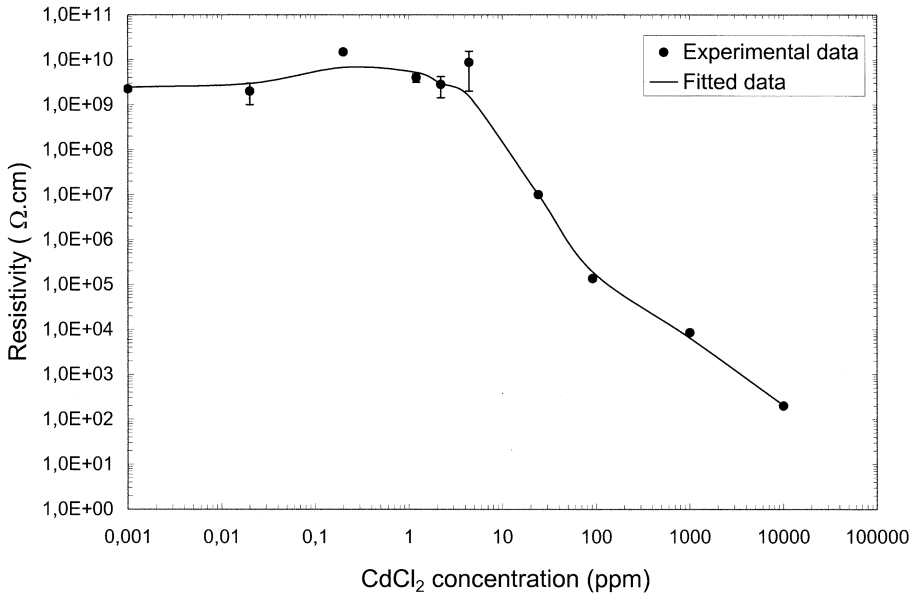

Fig. 10. Resistivity variation versus $CdCl_2$ concentrations.

the impurities diffusing during the thermal treatment can then induce the appearance of the defect band (0.3–0.4 eV).

Level P4: With a precision of 0.02 eV, it seems that this level is more a band than a single level. The first level is located at

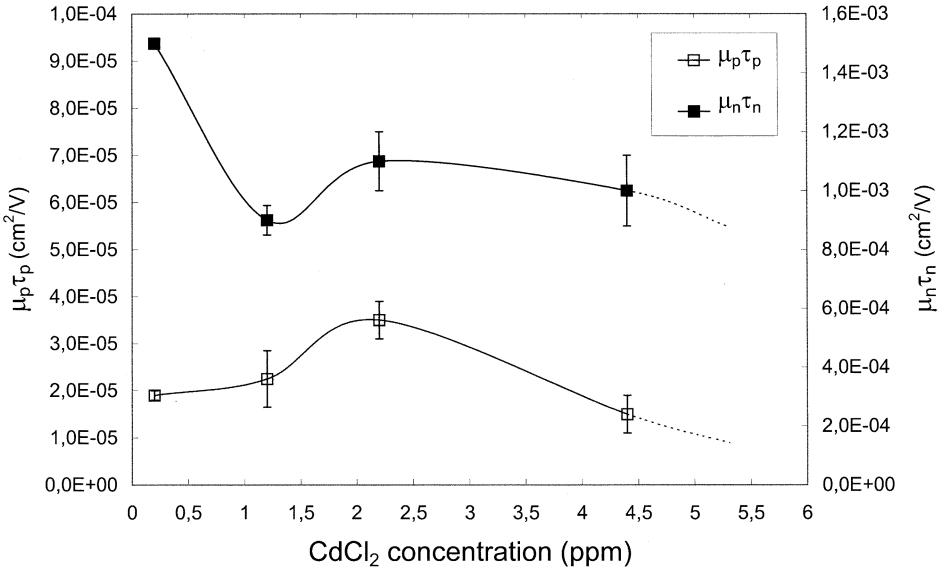

Fig. 11. Variation of $\mu\tau$ product of electrons and holes instead $CdCl_2$ concentrations.

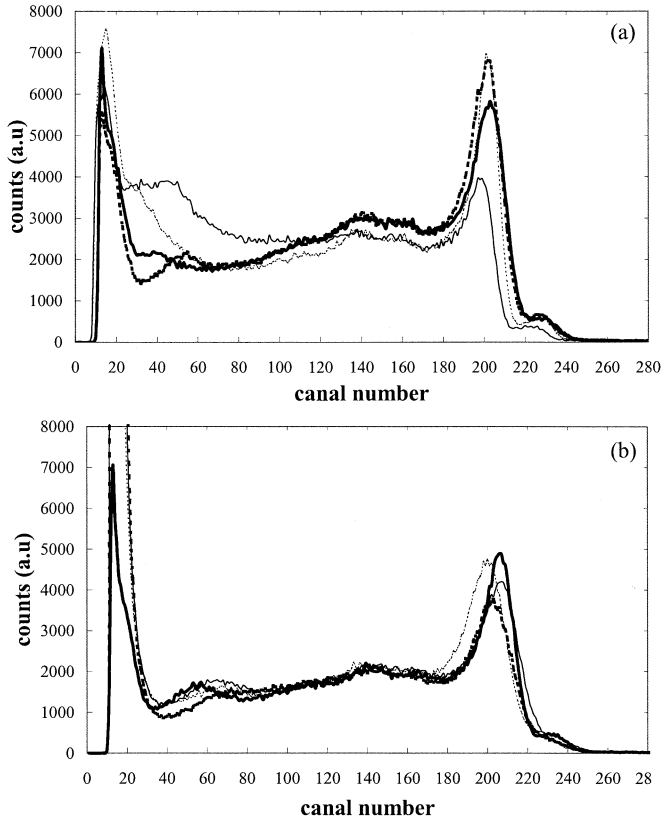

Fig. 12. ^{57}Co spectra in different detectors (a) before annealing and (b) after annealing at T:460 °C and with 2.2 ppm of $CdCl_2$ concentration.

0.4 eV. That we have found after vacuum annealing, ion irradiation, hydrostatic elastic pressures and so. It can be confidently attributed then to a V_{Cd} probably ionized with a single charge [10], [12], [15], [16]. On the other hand, Lischka *et al.* [17] found a level at ~0.43 eV, highly correlated to Fe that had been introduced. In our conditions, with annealing higher than the cadmium sublimation temperature that favors the formation of V_{Cd}, while if Fe and others transition metals are present in our low purity $CdCl_2$ (3N) that favors their diffusion [Fig. 9(c)–(d)], both effects increase this 0.4 band concentration.

Level P5: This is a donor level, located at 0.52 eV and identified by the TEES method. It is present only in annealing CdTe:Cl samples under a specific $CdCl_2$ concentration [Fig. 9(c)]. Laash *et al.* found a donor defect at 0.56 eV and attributed it to (Cd_i) [18].

Level P6: This is identified at $E_v + 0.6$ eV and is present in CdTe:Cl after the annealing. Höschl *et al.* attributed this defect to V_{Cd} [19]. Castaldini *et al.* [16] found a donor level at 0.64 eV both after and before the thermal treatment, and attributed it to a double charged donor (Cd_i).

In our case, this level is present when the samples have a poor resistivity and detection spectrum. It can probably be assigned to a V_{Cd}. This fact is due to the thermal treatment. At the high annealing temperature, the complex defects related to V_{Cd} and metallic impurities (P1, P2) dissociate and two new defects, one around 0.3 eV and the other at 0.6 eV appear. When the band (0.3–0.4 eV) concentration that is assigned to doping by metallic impurities increases the concentration of the 0.6 eV level increases too (Figs. 5 and 9). On the other hand, this level can be responsible for the sample polarization and plays a significant role on the resistivity value. Simulation of the resistivity versus donor and acceptor defects shows that the presence of a deep acceptor level like 0.6 or 0.7 eV in addition to the 0.9-eV level perturbs the compensation process and decreases the resistivity [20].

Level P7: This level, located at $E_v + 0.76$ eV, is present sometimes both before and after the annealing and has been attributed to an acceptor complex involving the native V_{Cd} defect and an impurity [14], [21], [22]. Its is sometimes present in samples that have poor resistivity and $\mu\tau$ product. It can influence these electrical parameters.

Levels $P9_0$ and $P9_1$: These are found at $E_c - 0.86$ eV and $E_c - 0.9$ eV. The $P9_1$ level is present always before annealing and sometimes after annealing while the $P9_0$ is present sometimes in annealed samples and especially in samples with a

lower resistivity. The origin of this defect is not well known, Lischka *et al.* found a level at 0.92 eV and attributed it to N_i^+/N_i^{3+} [17], while Hofmann *et al.* [23] attributed it to a vanadium impurity and located at 0.93 eV. Von Bardeleben *et al.* found a defect level at 0.95 eV and attribute it to germanium impurity [24]. A level at $E_c - 0.85$ eV was found by Photo-EPR and attributed to Sn [25], while Kremer *et al.* [26] found the same defect at $E_c - 0.9$ eV by using the DLTS method.

In fact, the presence of a deep level located near the mid gap necessarily involves the Fermi-level process which takes place in semi-conductor materials such as CdTe:Cl. This level plays an importance role on the shallow level compensation process [20]. The same authors show that one needs a donor level like 0.9 eV to compensate the acceptor shallow levels and, therefore, to reach the highest resistivity $(2 - 5 \times 10^9\ \Omega.\text{cm})$ for the CdTe:Cl material.

IV. Conclusion

Annealing under vacuum pressure induces the formation of vacancy defects such as V_{Cd} and V_{Te}, in which case the degradation of both the resistivity of the materials and the detection performance. But annealing under argon pressure results in an increase of the resistivity and an improvement of both the detection performance and the $\mu\tau$ product because this lowers the Cadmium sublimation kinetics. But on the other hand, the materials are still not uniform enough. The annealing under $CdCl_2$ with a concentration of 2.2 ppm, leads to an improvement of the performance detection and the $\mu\tau$ product too, and the more important factor; the uniformity of the materials in both precipitate parameters and electrical properties.

On the other hand, the investigation of the defects shows the importance of the donor deep level such as 0.9 eV on the compensation of the acceptor shallow levels. The influence of the 0.6-eV level on the electrical characteristics of the material and its assignment to probably a cadmium vacancy have been demonstrated.

References

[1] J. H. Greenberg, "P-T-X phase equilibrium and vapor pressure scanning of nonstoichiometry in CdTe," *J. Cryst. Growth*, vol. 161, no. 1–4, pp. 1–11, 1996.

[2] A. Zumbiehl, M. Hage Ali, M. Ayoub, R. Regal, J. M. Koebel, and P. Siffert, "Study of the homogeneity of CdTe-THM monolithic nuclear detector arrays: The role of electron lifetime and leakage current," *IEEE Trans. Nucl. Sci.*, vol. 49, pp. 1254–1257, June 2002.

[3] M. Ayoub, M. Hage Ali, J. M. Koebel, R. Régal, C. Rit, F. Klotz, and P. Siffert, "Real defect concentration measurements of nuclear detector materials by combination of PICTS and SCLC methods," *Mater. Sci. Eng.*, vol. B83, pp. 173–179, 2001.

[4] M. Samimi, B. Biglari, M. Hage Ali, J. M. Koebel, and P. Siffert, "About the origin of the 0.15 to 0.20 eV defect level in cadmium telluride," *Phys. Status Solidi*, vol. A100, pp. 251–258, 1987.

[5] B. M. Vul, V. S. Vavilov, V. S. Ivanov, V. B. Stopachinskii, and V. A. Chapnin, "Investigation of doubly charged acceptors in cadmium telluride," *Sov. Phys. Semicond.*, vol. 6, no. 8, pp. 1255–1260, 1973.

[6] N. V. Agrinskaya, E. N. Arkadeva, and O. A. Matveev, "Donor-cadmium vacancy associations in cadmium telluride," *Sov. Phys. Semicond.*, vol. 5, pp. 347–352, 1971.

[7] C. Canali, G. Ottaviani, R. O. Bell, and F. V. Wald, "Self-compensation in CdTe," *J. Phys. Chem. Solids*, vol. 35, pp. 1405–1413, 1974.

[8] B. K. Meyer, W. Stadler, and D. M. Hofmann, "On the nature of the deep 1.4 eV emission bands in CdTe-a study with photoluminescence and ODMR spectroscopy," *J. Cryst. Growth*, vol. 117, pp. 656–659, 1992.

[9] K. Suziki, S. Seto, A. Tanaka, and M. Kawashima, "Carrier drift mobilities and PL spectra of high resistivity cadmium telluride," *J. Cryst. Growth*, vol. 101, pp. 859–863, 1990.

[10] M. Fiederle, D. Ebling, C. Eiche, D. M. Hofmann, M. Salk, W. Stadler, K. W. Benz, and B. K. Meyer, "Comparison of CdTe, $Cd_{0.9}Zn_{0.1}Te$ and $CdTe_{0.9}Se_{0.1}$ crystals: application of γ and X-ray detectors," *J. Cryst. Growth*, vol. 138, pp. 529–533, 1994.

[11] B. K. Meyer, P. Omling, E. Weigel, and G. Muller-Vogt, "F center in CdTe," *Phys. Rev.*, vol. B46, pp. 15 135–15 138, 1992.

[12] W. Stadler, D. M. Hofmann, H. C. Alt, T. Mutschik, and B. K. Meyer, "Optical investigations of defects in $Cd_{1-x}Zn_xTe$," *Phys. Rev.*, vol. B51, pp. 10 619–10 630, 1995.

[13] V. P. Zayachkivskii, A. V. Savitskii, E. S. Nikonyunk, M. S. Kitsa, and V. V. Matlak, "Energy spectrum of capture levels in germanium-doped cadmium telluride," *Sov. Phys. Semicond.*, vol. 8, pp. 675–676, 1974.

[14] M. Hage Ali and P. Siffert, "Status of semi-insulating cadmium telluride for nuclear radiation detectors," *Nucl. Instrum. Methods Phys. Res.*, vol. A322, pp. 313–323, 1992.

[15] F. A. Kröger, "The defect structure of CdTe," *Rev. Phys. Appl.*, vol. 206, no. T12, N2, pp. 205–210, 1977.

[16] A. Castaldini, A. Cavallini, and B. Fraboni, "Deep energy levels in CdTe and CdZnTe," *J. Appl. Phys.*, vol. 83, no. N4, pp. 2111–2126, 1998.

[17] K. Lischka, G. Brunthaler, and W. Jantsch, "Deep donor levels due to isolated Fe IN CdTe," *J. Cryst. Growth*, vol. 72, pp. 355–359, 1985.

[18] M. Laash, M. Schwarz, M. Joeger, C. Eiche, and M. Fiederle, "Characterization of cadmium telluride crystals grown by different techniques from the vapor phase," *J. Cryst. Growth*, vol. 146, pp. 125–129, 1995.

[19] P. Höschl, R. Grill, J. Franc, P. Moravec, and E. Belas, "Native defect equilibrium in semi-insulating CdTe(Cl)," *Mater. Sci. Eng. B*, vol. 16, pp. 215–218, 1993.

[20] A. Zumbiehl, S. Mergui, M. Ayoub, M. Hage Ali, A. Zearrai, K. Cherkaoui, G. Marrakchi, and Y. Darici, "Compensation origins in II-VI CZT materials," *Mater. Sci. Eng.*, vol. B71, pp. 297–300, 2000.

[21] P. Moravec, M. Hage Ali, L. Chibani, and P. Siffert, "Deep levels in semi-insulating CdTe," *Mater. Sci. Eng.*, vol. B16, pp. 223–227, 1993.

[22] T. Tabeke, J. Saraie, and H. Matsunami, "Detailed characterization of deep centers in CdTe: photoionization and thermal ionization properties," *J. Appl. Phys.*, vol. 53, pp. 457–469, 1982.

[23] D. M. Hofmann, W. Stadler, P. Christmann, and B. K. Meyer, "Defects in CdTe and $Cd_{1-x}Zn_xTe$," *Nucl. Instrum. Methods A*, vol. 380, pp. 117–120, 1996.

[24] H. J. Von Bardeleben, T. Arnoux, and J. C. Launay, "Intrinsic defects in photorefractive bulk CdTe and ZnCdTe," *J. Cryst. Growth*, vol. 197, pp. 718–723, 1999.

[25] W. Jantsch and W. Hendorfer, "Characterization of deep levels in CdTe by photo-EPR and related techniques," *J. Cryst. Growth*, vol. 101, pp. 404–413, 1990.

[26] R. E. Kremer and W. B. Leigh, "Deep levels in CdTe," *J. Cryst. Growth*, vol. 86, pp. 490–496, 1988.